ACS Medicinal Chemistry Letters

Letter

Structure-property relationship studies of influenza A virus AM2-S31N proton channel blockers

Yanmei Hu, Raymond Kin Hau, Yuanxiang Wang, Peter Tuohy, Yongtao Zhang, Shuting Xu, Chunlong Ma, and Jun Wang

ACS Med. Chem. Lett., **Just Accepted Manuscript** • DOI: 10.1021/acsmedchemlett.8b00336 • Publication Date (Web): 03 Oct 2018

Just Accepted

ACS Publications

is published by the American Chemical Society. 1155 Sixteenth Street N.W., Washington, DC 20036

Structure-property relationship studies of influenza A virus AM2-S31N proton channel blockers

Yanmei Hu,[†,#] Raymond Kin Hau,[†,#] Yuanxiang Wang,[†] Peter Tuohy,[‡] Yongtao Zhang,[‡] Shuting Xu,[‡] Chunlong Ma,[†] Jun Wang[†,*]

[†]Department of Pharmacology and Toxicology, College of Pharmacy, The University of Arizona, Tucson, Arizona 85721, United States
[‡]Department of Chemistry and Biochemistry, The University of Arizona, Tucson, Arizona 85721, United States
[#]Yanmei Hu and Raymond Kin Hau contributed equally to this work

Keywords*: Influenza A virus, AM2 proton channel, AM2-S31N inhibitor, microsomal stability, antiviral.*

ABSTRACT: Majority of current circulating influenza A viruses carry the S31N mutation in their M2 genes, rendering AM2-S31N as a high profile antiviral drug target. With our continuous interest in developing AM2-S31N channel blockers as novel anti-virals targeting both oseltamivir-sensitive and –resistant influenza A viruses, we report herein the structure-property relationship studies of AM2-S31N inhibitors. The goal was to identify lead compounds with improved microsomal stability and membrane permeability. Two lead compounds, **10d** and **10e**, were found to have high mouse and human liver microsomal stability ($T_{1/2}$ > 145 min) and membrane permeability (>200 nm/s). Both compounds also inhibit both currently circulating oseltamivir-sensitive and –resistant human influenza A viruses (H1N1 and H3N2) with EC_{50} values ranging from 0.4 to 2.8 μM and a selectivity index of >100. We also showed for the first time that AM2-S31N channel blockers such as **10e** inhibited influenza virus replication at both low and high multiply of infection (10^2 –10^6 pfu/ml) and the inhibition was not cell type dependent. Overall, these studies have identified two promising lead candidates for further development as antiviral drugs against drug-resistant influenza A viruses.

Influenza viruses are negative sense, segmented RNA viruses that are the causative agents for annual influenza epidemic and sporadic influenza pandemics.[1] Despite the availability of small molecule antivirals and influenza vaccines, there is an influenza season every year. More concerning is the emerging of influenza pandemic outbreaks that normally occur every 10 to 20 years.[2] Part of explanation for the reoccurring influenza virus infection might be because influenza virus not only infects human, but also many animals such as swine, migrating birds, chicken, horse, sea lions, etc. As such, there are multiple sources where human can contract the virus. When healthy immunocompetent adults are infected with seasonal influenza viruses, the symptoms are normally mild and it is rarely fatal.[3] Therefore, it might be somewhat surprising to learn that influenza virus infection is currently listed among the top-ten leading causes of deaths in the United Sates.[4] The number of influenza virus-related mortality actually surpasses that of breast cancer. There are several factors that might contribute to the surprising death toll of influenza virus infection: (1) influenza virus is transmissible through the airways and can be quickly spread among humans. In each seasonal influenza epidemic, an estimate of 10-20% of the population are infected; (2) Mortality rate of influenza virus infection among people in high-risk groups is high.[5] They include seniors 65 years or older, people with chronic diseases such as cardiovascular diseases, diabetes, and high blood pressure, and people with compromised immune system. In such cases, influenza virus infection normally serves as a trigger of these pre-existing conditions. Overall influenza virus infection is a persistent public health concern that cannot be possibly ignored.

Currently there are two classes of FDA-approved small molecule influenza antivirals[6]: (1) adamantanes such as amantadine and rimantadine. They are channel blockers of the influenza virus AM2 proton channel and inhibit the early stage of viral replication by blocking the virus uncoating. (2) neuraminidase (NA) inhibitors such as oseltamivir, zanamivir, and peramivir. They are mimics of sialic acid and inhibit the late stage of viral replication by blocking the virus egress. Resistance to both classes of drugs now necessitates the development of newer influenza antivirals.[7] Majority of influenza A viruses (>95%) are now resistant to adamantanes due to the AM2-S31N mutation in their M2 genes, and CDC no longer recommends the use of adamantanes in the prophylaxis and treatment of influenza virus infection. Resistance to oseltamivir has been continuously reported, and more alarmingly, the 2007-2009 seasonal influenza virus circulating in North American and Japan was completely resistant to oseltamivir due to the H275Y mutation in it NA gene.[7-8] To tackle these drug-resistant viruses, several drug candidates are currently in development [6, 9] which include both direct-acting antivirals such as the PA (polymerase acidic protein) endonuclease inhibitor baloxavir marboxil (approved in Japan and in late stage clinical trial in U.S.), polymerase inhibitor T-705 and PB2 inhibitor JNJ-63623872, as well as host-targeting antivirals such as nitazoxanide and DAS181. In addition, a large number of other drug targets are also actively pursued in the early-stage of development.[10]

To design novel antivirals that are active against both oseltamivir-sensitive and –resistant influenza A viruses, we focus on targeting the influenza AM2-S31N proton channel.[14-16] AM2-S31N is a high profile antiviral drug target and more than 95% of current circulating influenza A viruses carry this mutation.[17] Therefore AM2-S31N channel blockers are expected to inhibit both oseltamivir-sensitive and –resistant influenza A viruses. As a proof-of-concept, we have shown that our rationally designed AM2-S31N inhibitors not only have potent channel blockage, but also effective antiviral activity against multiple human influenza A viruses that are in circulation in recent years, including both H1N1 and H3N2 viruses that are resistant to either amantadine, oseltamivir, or both.[14-16] Importantly, the newly developed AM2-S31N inhibitors showed a higher genetic barrier to drug resistance than amantadine, and drug resistance only emerged under high drug selection pressure after several passages.[18-19] To further advance these promising lead compounds to in vivo mice model studies and prove their in vivo antiviral efficacy, we report herein our progress in profiling the metabolism stability of previous reported AM2-S31N inhibitors. One candidate, compound **4**, was found to have good metabolic stability. Subsequent structure-activity and -property studies led to the discovery of two lead compounds, **10d** and **10e**, that have a long half-life in mouse and human liver microsomes ($T_{1/2}$ > 145 min) as well as a high membrane permeability (Pe > 200 nm/s). Both compounds **10d** and **10e** showed improved selectivity index than compound **4**. Importantly, compounds **10d** and **10e** retain potent antiviral activity against both oseltamivir-sensitive and –resistant human H1N1 and H3N2 influenza A viruses (EC_{50} = 0.4–2.8 μM), rendering them as promising candidates for the next step in vivo metabolic and efficacy studies in mice.

We have discovered several classes of adamantly-containing AM2-S31N inhibitors based on structure-guided design and medicinal chemistry optimization.[11-12, 14-16, 20] Representative examples of most potent AM2-S31N inhibitors were shown in Table 1. They had single to submicromolar efficacy in inhibiting AM2-S31N-containing human influenza A viruses, including current circulating H1N1 and H3N2 strains. As a first step to profile the in vitro absorption, distribution, metabolism, excretion, and toxicity (ADMET) properties, we first tested their **Table 1. Microsomal stability profiling of previously reported AM2-S31N inhibitors.**

Compound structure and ID	MLM 0.5	
	$T_{1/2}$ (min)	$CL_{int(liver)}$ (ml/min/kg)
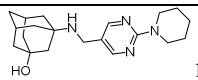 **1** (ref[11])	19.4	282.7
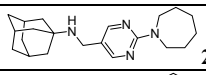 **2** (ref[11])	0.8	6762.7
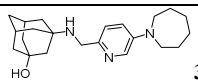 **3** (ref[11])	22.1	248.3
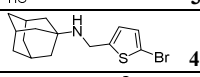 **4** (ref[12])	> 145	< 38.0
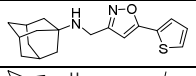 **5** (ref[13])	1.0	5290.9
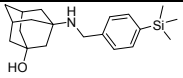 **6** (ref[14])	4.4	566

microsomal stability in mouse liver microsomes. Surprisingly, all compounds except compound **4** had low microsomal stability ($T_{1/2}$ < 30 min) (Table 1), precluding them from further progression. Encouragingly, compound **4** showed good microsomal stability with a $T_{1/2}$ > 145 min, and the predicted liver clearance is less than 38.0 ml/min/kg. Therefore, compound **4** was selected as a lead compound for further optimization.

Given the promising results of compound **4**, a library of thiophene containing AM2-S31N inhibitors were synthesized and tested for channel blockage, antiviral activity, cellular cytotoxicity and microsomal stability. Specifically, two series of new adamantane analogs, the mono-aryl adamantanes (**10a-10i**) and the bis-aryl adamantanes (**12a-12i**), were designed and synthesized (Figure 1).

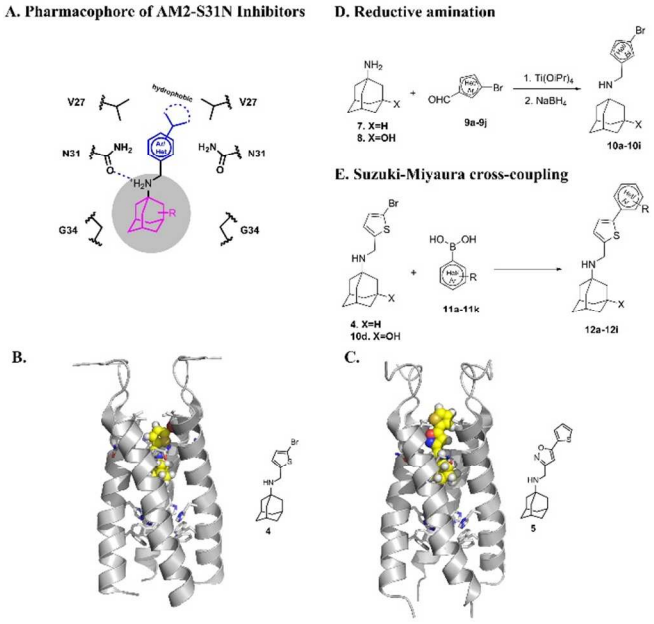

Figure 1. Design and synthesis of AM2-S31N inhibitors. (A) Pharmacophore of AM2-S31N inhibitors. Adamantane cage fits in the hydrophobic cavity formed by Gly34, the ammonium linker forms a hydrogen bond with the Asn31 side chain carbonyl, and the substitution on the aryl group forms hydrophobic interactions with the Val27 side chain. (B) Solution NMR structure of mono-aryl AM2-S31N inhibitor **4** in complex with AM2-S31N (19-49) (PDB: 2MUV).[12] (C) Solution NMR structure of bis-aryl AM2-S31N inhibitor **5** in complex with AM2-S31N (19-49) (PDB: 2LY0).[13] (D) Synthesis of mono-aryl adamantanes by reductive amination. (E) Synthesis of bi-aryl adamantanes by Suzuki-Miyaura cross-coupling reaction.

The design was based on the AM2-S31N inhibitor pharmacophore (Figure 1A), which was derived from previous structure-activity relationship studies.[16] Both series of adamantane analogs (**10a-10i** and **12a-12i**) meet the requirements of the AM2-S31N pharmacophore. Therefore, it is likely that they will have potent channel blockage and antiviral activity. Representative examples of mono-aryl and bis-aryl AM2-S31N inhibitors are compounds **4** and **5**, respectively, and their binding modes to the AM2-S31N channel were determined by solution NMR as shown in Figures 1B and 1C, respectively.[12-13] The mono-aryl adamantanes were synthesized using our previously optimized reduction amination condition (Figure 1D),[21] and the yields range from 62% to 85%. The bis-aryl adamantanes were synthesized using the expeditious mi-

crowave-mediated Suzuki-Miyaura cross-coupling reaction (Figure 1E), and the yields range from 75% to 92%.

The challenge of structure-property relationship studies is that the ADMET properties need to be optimized without negatively affecting the channel blockage and antiviral efficacy. In the first step, we focus on optimizing the mouse liver microsomal stability because mouse is a commonly used animal model for the evaluation of the in vivo antiviral efficacy of influenza antivirals.[22-23] Changing the bromide in compound **4** with iodide resulted in compound **10a**, which had improved antiviral activity (EC_{50} = 1.0 ± 0.1 μM vs 2.9 ± 0.8 μM), but drastically reduced microsomal stability ($T_{1/2}$ = 24.5 min vs >145 min) (Table 2). The selenium analog **10b** had similar antiviral activity as the thiophene **4**, but it was less metabolically stable ($T_{1/2}$ = 32.1 min vs >145 min). Replacing the adamantane in **4** with ring-expanded adamantane gave compound **10c**, which had increased antiviral activity (EC_{50} = 0.6 ± 0.1 μM vs 2.9 ± 0.8 μM), but drastically reduced microsomal stability ($T_{1/2}$ = 9.1 min vs >145 min). In contrast, replacing adamantane in compound **4** with hydroxyl-adamantane yielded compound **10d** that not only had improved antiviral activity (EC_{50} = 1.1 ± 0.2 μM vs 2.9 ± 0.8 μM), but also high microsomal stability ($T_{1/2}$ >145 min). Encouraged by this result, we then synthesized the iodide analog **10e**. It was found that the iodide analog **10e** retained the potent antiviral activity and high microsomal stability (EC_{50} = 0.9 ± 0.1 μM, $T_{1/2}$ >145 min). Both compounds **10d** and **10e** also had an improved selectivity index than compound **4**. Two additional bromothiophene analogs **10f** and **10g** had reduced antiviral activity compared to compound **10d**, and compound **10f** was also less metabolically stable than **10d** ($T_{1/2}$ = 100.8 min vs >145 min). The bromothiazole analogs **10h** and **10i** had drastically reduced channel blockage and antiviral activity, showing less than 40% channel inhibition at 100 μM. For the bis-aryl adamantane analogs **12a-12i**, only compounds **12b** and **12f** had comparable antiviral activity as compound **10d**. The antiviral EC_{50} values of **12b** and **12f** were 2.1 ± 0.2 μM, and 2.5 ± 0.8 μM respectively. However both **12b** and **12f** had reduced selectivity index than compound **10d**, therefore they were not further pursued. All other bis-aryl compounds (**12a**, **12c**, **12d**, **12e**, **12g**, **12h**, and **12i**) had significantly reduced antiviral activity as shown by the values of percentage plaque formation at 10 μM. All compounds (**10a-10i** and **12a-12i**) were also tested against the wild-type (WT) AM2 channel, and compounds **4**, **10a**, and **10c** were found to have potent channel blockage against AM2-WT (>77% inhibition at 100 μM). Compound **10b** had moderate activity (56.1 ± 0.8% inhibition at 100 μM), and all other compounds were inactive. In summary, through the structure-property relationship studies, we identified two lead compounds **10d** and **10e** that had potent channel blockage, antiviral activity, a high selectivity index, and optimal microsomal stability.

The membrane permeability of the two lead compounds **10d** and **10e** was further profiled (Table 3). First, the membrane permeability and oral absorption of compounds **10d** and **10e** were predicted by the Schrödinger Glide QikProp program, and both compounds were predicted to have high membrane permeability and oral absorption (Table 3). Next, to experimentally determine their membrane permeability, compounds **10d** and **10e** were tested in the parallel artificial membrane permeability assay (PAMPA), which is commonly used as an in vitro model of passive, transcellular permeation. Both compounds **10d** and **10e** showed high membrane permeability with Pe greater than 200 nm/s in the Egg-PAMPA assay, indicating they can passively diffuse through the transcellular membrane. Both compounds **10d** and **10e** also didn't violate the Lipinski rule of five. The microsomal stability of compounds **10d** and **10e** was further confirmed in human liver microsomal stability test and both compounds **10d** and **10e** were found to have a long half-life with $T_{1/2}$ > 145 mins. Taken together, compounds **10d** and **10e** appear to be promising leads for further development.

One of the major therapeutic advantages of AM2-S31N inhibitors is that they have no cross-resistance with neuraminidase inhibitors such as oseltamivir.[18] Therefore they are expected to have potent antiviral activity against both oseltamivir-sensitive and –resistant influenza A viruses since more than 95% of current circulating influenza A viruses have AM2-S31N mutation in their M2 genes. To prove this hypothesis, we tested the antiviral activity of compounds **10d** and **10e** against several human influenza A viruses, including both H1N1 and H3N2 strains (Table 4). These viruses were chosen because of their clinical relevance, and similar viruses are circulating among humans in recent years. All viruses contain the AM2-S31N mutation in their M2 genes and are resistant to amantadine. In addition, the four oseltamivir-resistant strains encode the H275Y mutant in their neuraminidase gene which confer to their resistance to oseltamivir. It was found that compounds **10d** and **10e** inhibited all seven influenza A viruses with EC_{50} values ranging from 0.4 μM to 2.8 μM.

The antiviral activity of compound **10e** was further validated when MDCK cells were infected with the A/California/07/2009 (H1N1) or the A/Wisconsin/67/2005 (H3N2) virus at high MOIs, a condition which mimics the late stage of treatment when the virus was already amplified in the host. It was found that compound **10e** significantly suppressed the viral replication when MOI was as high as 10^6 pfu/ml for both influenza strains (Figure 2). In contrast, oseltamivir carboxylate was only effect at low MOIs (10^1 to 10^3 pfu/ml) and was not effective at high MOIs (10^4-10^6 pfu/ml). Overall compound **10e** showed potent inhibition against human H1N1 and H3N2 influenza A strains at both low and high MOIs.

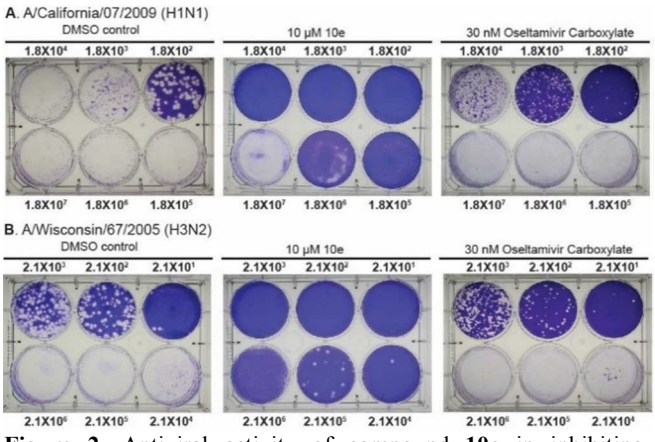

Figure 2. Antiviral activity of compound **10e** in inhibiting A/California/07/2009 (H1N1) and A/Wisconsin/67/2005 (H3N2) viruses at different MOIs (10^1-10^6 pfu/ml). Confluent MDCK cells were infected with either A/California/07/2009 (H1N1) virus (A) or the A/Wisconsin/67/2005 (H3N2) virus (B) for 1h at 4 °C follow by 1h at 37 °C. Avicel overlay containing 10 μM of compound **10e** was added to the cell and the plate was incubated for 46 h and 56 h for A and B, respectively. Cells were stains with crystal violet dye. The images shown were representative results from two repeats.

Table 2. Channel blockage, antiviral activity, cytotoxicity, and mouse liver microsomal stability of AM2-S31N inhibitors.

Structure/Compound ID	TEVC assay[a] (% S31N channel inhibition)	TEVC assay[a] (% WT channel inhibition)	% plaque formation at 10 μM[b]	EC_{50} (μM) A/California/07/2009 (H1N1)[b]	CC_{50} (μM) MDCK cells[c]	$T_{1/2}$ (min)	$CL_{int(liver)}$ (ml/min/kg)
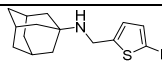 **4**	76.3 ± 2.5	77.2 ± 4.3	3.2 ± 0.5	2.9 ± 0.8	123.2 ± 8.6	>145	<38.0
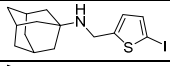 **10a**	78.5 ± 2.4	91 ± 1.6	1.8 ± 0.3	1.0 ± 0.1	70.2 ± 3.6	24.5	223.6
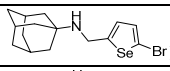 **10b**	70.6 ± 2.2	56.1 ± 0.8	0	2.2 ± 1.9	82.1 ± 5.2	32.1	170.7
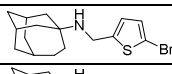 **10c**	72.6 ± 1.4	86.5 ± 0.3	0	0.6 ± 0.1	43.1 ± 2.8	9.1	603.6
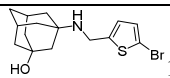 **10d**	64.7 ± 3.5	11.4 ± 1.1	3.9 ± 1.2	1.1 ± 0.2	238.1 ± 2.1	>145	<38.0
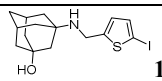 **10e**	75.6 ± 1.2	3.2 ± 1.5	2.5 ± 1.9	0.9 ± 0.1	317.4 ± 12.0	>145	<38.0
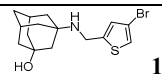 **10f**	56.6 ± 1.3	6.5 ± 1.4	31.4 ± 0.5	3.1 ± 0.3	380.7 ± 24.9	100.8	54.5
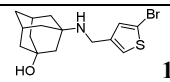 **10g**	48.3 ± 0.5	1.9 ± 0.9	31.3 ± 0.5	5.1 ± 0.6	363.7 ± 18.3	N.T.	N.T.
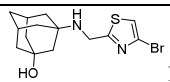 **10h**	36.0 ± 0.4	3.9 ± 0.0	108.0 ± 1.8	N.T.	N.T.	N.T.	N.T.
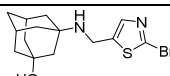 **10i**	33.5 ± 1.2	2.7 ± 0.9	102.1 ± 0.4	N.T.	N.T.	N.T.	N.T.
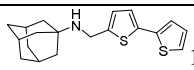 **12a**	86.1 ± 1.2	17.9 ± 3.2	58.5 ± 3.2	12.16 ± 1.11	19.5 ± 2.0	2.8	1939.0
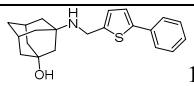 **12b**	84.6 ± 1.2	0.3 ± 0.2	27.9 ± 0.7	2.1 ± 0.2	80.5 ± 5.5	N.T.	N.T.
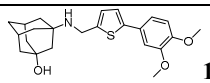 **12c**	37.6 ± 0.6	0	67.5 ± 1.9	N.T.	N.T.	N.T.	N.T.
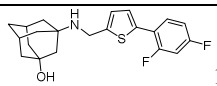 **12d**	74.5 ± 1.1	0	44.1 ± 1.1	N.T.	N.T.	N.T.	N.T.
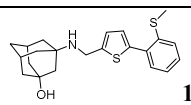 **12e**	73.4 ± 1.8	0	47.7 ± 1.2	N.T.	N.T.	N.T.	N.T.
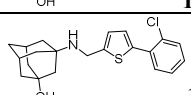 **12f**	78.7 ± 1.3	0	20.4 ± 1.4	2.5 ± 0.8	65.2 ± 5.7	N.T.	N.T.
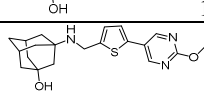 **12g**	4.4 ± 2.4	0	74.0 ± 0.5	N.T.	N.T.	N.T.	N.T.
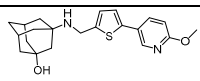 **12h**	68.3 ± 1.2	0	40.5 ± 1.0	N.T.	N.T.	N.T.	N.T.
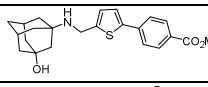 **12i**	64.3 ± 2.4	0	52.0 ± 0.7	N.T.	N.T.	N.T.	N.T.
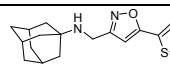 **5**	90.3 ± 3.4	11.2 ± 1.3	0	0.3 ± 0.1	100	1.0	5290.9

[a]Values represent the mean of three independent measurements ± standard deviation. Compounds were tested at 100 μM concentration. [b]Antiviral activity was tested with the A/California/07/2009 (H1N1) virus, which contains the AM2-S31N mutant, in plaque assay. Values represent the mean of two independent measurements ± standard deviation. [c]Cytotoxicity was tested by incubating MDCK cells with compounds for 48 h and the cells were stained with neutral red.[24] N.T. = not tested.

Table 3. PK predictions, membrane permeability, physiochemical properties, and mouse microsomal stability of lead compounds 10d and 10e.

Compound structure	Predicted values by Glide QikPropa	Egg-PAMPA Permeability (nm/s)	Lipinski rule of five[a]	Mouse liver microsome stability $T_{1/2}$ (min)	Human liver microsome stability $T_{1/2}$ (min)
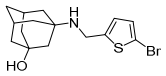 **10d**	Caco-2: 892 nm/s MDCK: 2163 nm/s (<25 poor, >500 great) % human oral absorption in GI: 100 (<25% is poor)	252.814	M.W. = 342.3 HBD = 2 HBA = 3 cLogP = 3.69	>145	>145
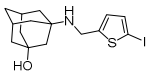 **10e**	Caco-2: 892 nm/s MDCK: 2374 nm/sec (<25 poor, >500 great) % human oral absorption in GI: 100 (<25% is poor)	204.422	M.W. = 389.3 HBD = 2 HBA = 3 cLogP = 3.80	>145	>145

[a]Membrane permeability and cLogP were calculated by the Schrödinger Glide QikProp program.

Table 4. Antiviral activity of compounds 10d and 10e in inhibiting oseltamivir-sensitive and –resistant influenza A viruses.

Compound structures	A/California/07/2009 (H1N1) EC_{50}	A/Switzerland/9715293/2013 (H3N2) EC_{50}	A/Wisconsin/67/2005 (H3N2) EC_{50}	A/Washington/29/2009 (H1N1) EC_{50}	A/Texas/04/2009 (H1N1) EC_{50}	A/North Carolina/29/2009 (H1N1) EC_{50}	A/Denmark/528/2009 (H1N1) EC_{50}	CC_{50} MDCK cells
	Amantadine-resistant (AM2-S31N) Oseltamivir-sensitive			Amantadine-resistant (AM2-S31N) Oseltamivir-resistant (H275Y)				
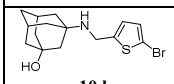 **10d**	1.1 ± 0.2 µM	0.5 ± 0.1 µM	1.4 ± 0.1 µM	0.7 ± 0.1 µM	0.6 ± 0.1 µM	2.8 ± 0.2 µM	2.0 ± 0.3 µM	238.1 ± 2.1 µM
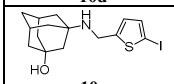 **10e**	0.9 ± 0.1 µM	0.7 ± 0.1 µM	0.8 ± 0.1 µM	0.4 ± 0.1 µM	0.6 ± 0.1 µM	1.1 ± 0.2 µM	0.7 ± 0.1 µM	317.4 ± 12.0 µM
Oseltamivir Carboxylate	2.4 ± 0.3 nM	12.3 ± 5.2 nM	2.5 ± 0.5 nM	> 200 nM	> 200 nM	>200 nM	> 200 nM	> 20 µM

To test whether the antiviral efficacy of compound **10e** is cell-type dependent, we performed viral titer reduction assay using the A/California/07/2009 (H1N1) virus and the A549 cells. In this assay, confluent A549 cells were infected with the A/California/07/2009 (H1N1) virus at MOI of 0.001, and the cell culture supernatant was collected at 24, 48, and 72 hours post infection and the viral titer was quantified by plaque assay. Compared with the DMSO control, treatment with 10 µM of compound **10e** significantly reduced the viral titers of 1.8, 2.1, and 2.9 log10 unites at 24, 48, and 72 hrs, respectively (Figure 3). In comparison, oseltamivir carboxylate only delayed viral replication and showed no effect at 72 hpi under similar drug selection pressure (10-fold of EC_{50} value).

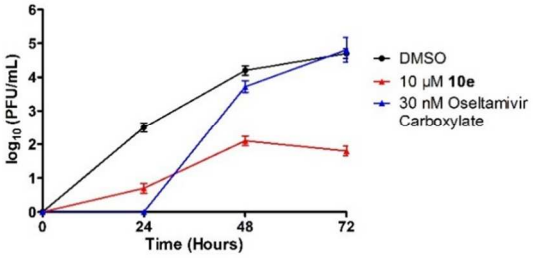

Figure 3. Antiviral activity of compound **10e** in inhibiting A/California/07/2009 (H1N1) virus replication in A549 cells. Confluent A549 cells were infected with A/California/07/2009 (H1N1) virus at MOI of 0.001. Supernatant was collected at 24, 48, and 72 hours post infection and the viral titer was quantified by plaque assay. The results shown were from two repeats.

The binding of compound **10e** in the AM2-S31N channel was modeled by the Schrödinger Glide standard precision docking program. In the energy minimized docking pose (Figure 4), compound **10e** fitted inside the channel with the thiophene group facing towards the N-terminal of the channel. The hydroxyl group from 10e forms a hydrogen bond with the backbone amide carbonyl from one of the helixes, and the ammonium from 10e forms another hydrogen bond with the side chain amide carbonyl from the neighboring helix. The iodothiophene substitution forms hydrophobic interactions with the V27 side chain methyls. Overall, the docking pose of compound **10e** is similar to that of compound 10e as shown in the solution NMR structure (PDB: 2MUV) (Figure 1b).

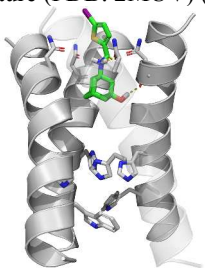

Figure 4. Docking model of compound **10e** in the transmembrane domain of AM2-S31N (PDB: 2LY0) [13]. The transparency of the front helix was set as 0.7 for clarity. Docking was performed using Schrödinger Glide standard precision.

Drug discovery is a lengthy and expansive endeavor,[25] and lead compounds can fail in any step during the early preclinical development phase or the later human clinical trials. Therefore, it is essential to provide additional backup compounds with favorable PK properties for the following in vivo animal and human studies. Herein we report our progress of optimizing the mouse microsomal stability and cell membrane permeability of thiophene-containing AM2-S31N inhibitors. Starting from a promising lead compound 4, we were able to identify two compounds **10d** and **10e** with improved antiviral efficacy and selectivity index. The optimized lead compounds

10d and **10e** retained high mouse liver microsomal stability ($T_{1/2}$ > 145 mins), had favorable membrane permeability in the PAMPA assay (Pe > 200 nm/s) as well as a high selectivity index (SI > 100). As a demonstration of the therapeutic value of AM2-S31N inhibitors, compounds **10d** and **10e** were found to have potent antiviral potency against several oseltamivir-sensitive and -resistant human influenza A viruses. Compound **10e** was also able to inhibit A/California/07/2009 (H1N1) and A/Wisconsin/67/2005 (H3N2) at MOIs ranging from 10^2 to 10^6 pfu/ml, and the antiviral activity of compound 10e was further confirmed in human A549 cell line. Taken together, the potent antiviral efficacy, a high selectivity index, a long half-life in mouse liver microsomes, and a high membrane permeability of the identified lead compounds **10d** and **10e** warrant their further development as orally bioavailable influenza antivirals. Indeed, several FDA-approved oral drugs such as rivaroxaban, chlorothen, brotizolam, and lornoxicam similarly contain halogen-deactivated thiophene,[26] which reassures continuous development of this series of compounds.

ASSOCIATED CONTENT

Supporting Information

The Supporting Information is available free of charge on the ACS Publications website.

Synthesis procedures, characterization of compounds; antiviral and cytotoxicity assay; electrophysiological assay; mouse microsomal stability assay; membrane permeability assay.

AUTHOR INFORMATION

Corresponding Author

* Email: junwang@pharmacy.arizona.edu. Tel: +1 (520)-626-1366.

Author Contributions

The manuscript was written through contributions of all authors. All authors have given approval to the final version of the manuscript. ‡These authors contributed equally.

Funding Sources

This research is supported by the startup funding from the University of Arizona and the NIH grant AI119187 to J. W.

ABBREVIATIONS

WT, wild type; DMEM, Dulbecco's modified eagle medium; MDCK, Madin–Darby Canine Kidney; TEVC, two-electrode voltage clamps.

REFERENCES

1. Webster, R. G.; Monto, A. S.; Braciale, T. J.; Lamb, R. A., *Textbook of Influenza*. Wiley: 2013.
2. http://www.flu.gov/pandemic/history/. Accessed on 09/28/2018.
3.https://www.cdc.gov/flu/professionals/acip/clinical.htm. Accessed on 09/28/2018.
4.https://www.cdc.gov/nchs/fastats/leading-causes-of-death.htm. Accessed on 09/28/2018.
5.https://www.cdc.gov/flu/about/disease/high_risk.htm. Accessed on 09/28/2018.
6. Shaw, M. L., The Next Wave of Influenza Drugs. *ACS Infect Dis* **2017**, *3*, 691-694.
7. Hurt, A. C., The epidemiology and spread of drug resistant human influenza viruses. *Curr Opin Virol* **2014,** *8*, 22-29.
8. Matsuzaki, Y.; Mizuta, K.; Aoki, Y.; Suto, A.; Abiko, C.; Sanjoh, K.; Sugawara, K.; Takashita, E.; Itagaki, T.; Katsushima, Y.; Ujike, M.; Obuchi, M.; Odagiri, T.; Tashiro, M., A two-year survey of the oseltamivir-resistant influenza A(H1N1) virus in Yamagata, Japan and the clinical effectiveness of oseltamivir and zanamivir. *Virol J* **2010,** *7*, 53.
9. Koszalka, P.; Tilmanis, D.; Hurt, A. C., Influenza antivirals currently in late-phase clinical trial. *Influenza Other Respir Viruses* **2017,** *11* (3), 240-246.
10. Loregian, A.; Mercorelli, B.; Nannetti, G.; Compagnin, C.; Palu, G., Antiviral strategies against influenza virus: towards new therapeutic approaches. *Cell Mol Life Sci* **2014,** *71* (19), 3659-3683.
11. Li, F.; Ma, C.; Hu, Y.; Wang, Y.; Wang, J., Discovery of Potent Antivirals against Amantadine-Resistant Influenza A Viruses by Targeting the M2-S31N Proton Channel. *ACS Infect Dis* **2016,** *2* (10), 726-733.
12. Wu, Y.; Canturk, B.; Jo, H.; Ma, C.; Gianti, E.; Klein, M. L.; Pinto, L. H.; Lamb, R. A.; Fiorin, G.; Wang, J.; DeGrado, W. F., Flipping in the pore: discovery of dual inhibitors that bind in different orientations to the wild-type versus the amantadine-resistant S31N mutant of the influenza A virus M2 proton channel. *J Am Chem Soc* **2014,** *136* (52), 17987-17995.
13. Wang, J.; Wu, Y.; Ma, C.; Fiorin, G.; Wang, J.; Pinto, L. H.; Lamb, R. A.; Klein, M. L.; Degrado, W. F., Structure and inhibition of the drug-resistant S31N mutant of the M2 ion channel of influenza A virus. *Proc. Natl. Acad. Sci. U. S. A.* **2013,** *110* (4), 1315-1320.
14. Hu, Y.; Wang, Y.; Li, F.; Ma, C.; Wang, J., Design and expeditious synthesis of organosilanes as potent antivirals targeting multidrug-resistant influenza A viruses. *Eur J Med Chem* **2017,** *135*, 70-76.
15. Li, F.; Hu, Y.; Wang, Y.; Ma, C.; Wang, J., Expeditious Lead Optimization of Isoxazole-Containing Influenza A Virus M2-S31N Inhibitors Using the Suzuki-Miyaura Cross-Coupling Reaction. *J Med Chem* **2017,** *60* (4), 1580-1590.
16. Li, F.; Ma, C.; DeGrado, W. F.; Wang, J., Discovery of Highly Potent Inhibitors Targeting the Predominant Drug-Resistant S31N Mutant of the Influenza A Virus M2 Proton Channel. *J Med Chem* **2016,** *59* (3), 1207-1216.
17. Dong, G.; Peng, C.; Luo, J.; Wang, C.; Han, L.; Wu, B.; Ji, G.; He, H., Adamantane-resistant influenza a viruses in the world (1902-2013): frequency and distribution of M2 gene mutations. *PLoS One* **2015,** *10* (3), e0119115.
18. Ma, C.; Zhang, J.; Wang, J., Pharmacological Characterization of the Spectrum of Antiviral Activity and Genetic Barrier to Drug Resistance of M2-S31N Channel Blockers. *Mol Pharmacol* **2016,** *90* (3), 188-198.
19. Musharrafieh, R.; Ma, C. L.; Wang, J., Profiling the in vitro drug-resistance mechanism of influenza A viruses towards the AM2-S31N proton channel blockers. *Antiviral Res* **2018,** *153*, 10-22.
20. Wang, Y.; Hu, Y.; Xu, S.; Zhang, Y.; Musharrafieh, R.; Hau, R. K.; Ma, C.; Wang, J., In Vitro Pharmacokinetic Optimizations of AM2-S31N Channel Blockers Led to the Discovery of Slow-Binding Inhibitors with Potent Antiviral Activity against Drug-Resistant Influenza A Viruses. *J Med Chem* **2018,** *61* (3), 1074-1085.
21. Wang, J.; Ma, C.; Wang, J.; Jo, H.; Canturk, B.; Fiorin, G.; Pinto, L. H.; Lamb, R. A.; Klein, M. L.; DeGrado, W. F., Discovery of novel dual inhibitors of the wild-type and the most prevalent drug-resistant mutant, S31N, of the M2 proton channel from influenza A virus. *J Med Chem* **2013,** *56* (7), 2804-2812.
22. Hu, Y.; Musharrafieh, R.; Ma, C.; Zhang, J.; Smee, D. F.; DeGrado, W. F.; Wang, J., An M2-V27A channel blocker demonstrates potent in vitro and in vivo antiviral activities against amantadine-sensitive and -resistant influenza A viruses. *Antiviral Res* **2017,** *140*, 45-54.
23. Smee, D.; Barnard, D., Methods for Evaluation of Antiviral Efficacy Against Influenza Virus Infections in Animal Models. In *Antiviral Methods and Protocols*, Gong, E. Y., Ed. Humana Press: 2013; Vol. 1030, pp 407-425.
24. Repetto, G.; del Peso, A.; Zurita, J. L., Neutral red uptake assay for the estimation of cell viability/cytotoxicity. *Nat Protoc* **2008,** *3* (7), 1125-1131.
25. DiMasi, J. A.; Grabowski, H. G.; Hansen, R. W., Innovation in the pharmaceutical industry: New estimates of R&D costs. *J Health Econ* **2016,** *47*, 20-33.
26. Scott, K. A.; Njardarson, J. T., Analysis of US FDA-Approved Drugs Containing Sulfur Atoms. *Top Curr Chem (Cham)* **2018,** *376* (1), 5.

TOC

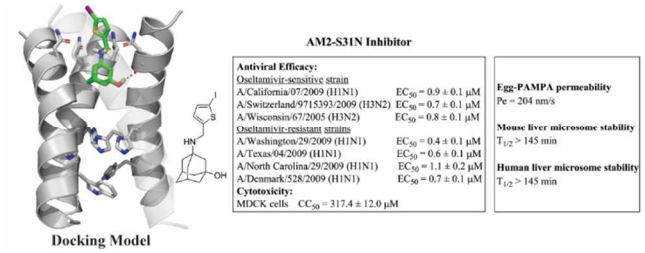
AM2-S31N Inhibitor
Antiviral Efficacy:
Oseltamivir-sensitive strain
A/California/07/2009 (H1N1) EC50 = 0.9 ± 0.1 μM
A/Switzerland/9715393/2009 (H3N2) EC50 = 0.7 ± 0.1 μM
A/Wisconsin/67/2005 (H3N2) EC50 = 0.8 ± 0.1 μM
Oseltamivir-resistant strains
A/Washington/29/2009 (H1N1) EC50 = 0.4 ± 0.1 μM
A/Texas/04/2009 (H1N1) EC50 = 0.6 ± 0.1 μM
A/North Carolina/29/2009 (H1N1) EC50 = 1.1 ± 0.2 μM
A/Denmark/528/2009 (H1N1) EC50 = 0.7 ± 0.1 μM
Cytotoxicity:
MDCK cells CC50 = 317.4 ± 12.0 μM
Egg-PAMPA permeability
Pe = 204 nm/s
Mouse liver microsome stability
T1/2 > 145 min
Human liver microsome stability
T1/2 > 145 min
HN
S
OH
Docking Model